Обзоры актуальных проблем нелинейной динамики

Изв. вузов «ПНД», т. 17, № 4, 2009 УДК 537.86:519.22

PATTERNS IN EXCITABLE DYNAMICS DRIVEN BY ADDITIVE DICHOTOMIC NOISE

X. Sailer, D. Hennig, and L. Schimansky-Geier

Pattern formation due the presence of additive dichotomous fluctuations is studied an extended system with diffusive coupling and a bistable FitzHugh–Nagumo kinetics. The fluctuations vary in space and/or time being noise or disorder, respectively. Without perturbations the dynamics does not support pattern formation. With proper dichotomous fluctuations, however, the homogeneous steady state is destabilized either via a Turing instability or the fluctuations create spatial nuclei of an inhomogeneous states. Finally, for purely static dichotomous disorder we find destabilization of homogeneous steady states for finite nonzero correlation length of the disorder resulting again in spatial patterns.

Keywords: FitzHugh–Nagumo, Turing pattern, dichotomic noise, additive noise.

Introduction

Several of the most prominent patterns observed in nature are due to a Turing instability [1, 2]. This phenomenon occurs when inhomogeneous perturbations of certain wavelength(s) cause destabilization of a homogeneous steady state. Recently a lot of interest was spent to the interaction of noise/disorder and nonlinearity [2–6]. Especially the possibility of inducing a pattern formation process by help of fluctuations has been studied, intensely [7–11]. As outcome of this research many various types of underlying deterministic dynamics support spatial structures and exhibit a Turing instability of their dynamic behavior if optimal noise is added. Especially excitability and bistability, where new time scales and new possible response is opened in the presence of noise are often studied objects for theoretical and experimental investigations [5].

The possibility of Turing-pattern formation induced by dichotomous fluctuations has been demonstrated recently in a series of papers [12–16]. The dichotomous fluctuations switch between two different dynamical systems each of which does not support Turing pattern formation, i.e. each undriven system possesses a pattern-free steady state. As result, it was just the switching between them that triggers the creation of spatial structures. Importantly to notice, that the authors have used dynamical models with either multiplicative dichotomous noise or switched between two distinct dynamics each having its own state dependency.

In the present study we investigate an extended array that locally possesses FitzHugh–Nagumo (FHN) dynamics. The FHN system is a prototypical model system exhibiting

both excitable and bistable behavior. Originally the FHN system was developed to describe nerve cell activity but achieves generality as one of the prototypical models for excitability and bistability [5, 17–21].

The dynamics is assumed to be subject to *additive* dichotomous driving varying either in space or in time or in both simultaneously [22]. More precisely, we illustrate that additive dichotomous driving in the excitable regime of the extended FHN system may act in a way that initially a single local inhomogeneity (single hump on the uniform rendered steady state background) is generated. This inhomogeneity acts as the core from which the pattern evolves throughout the whole space. The growth proceeds stepwise, i.e. with each switching new boundary layers are created adjacent to the core.

Also small Gaussian additive white noise is initially present to destabilize homogeneous states. Special emphasis is put on the influence of different correlation lengths and times of the dichotomic drive. Apart from obtaining regular pattern induced by additive driving we find a novel mechanism to generate them. Whereas previous works [12–16] operated with small correlation lengths or times we deal with forcing with intermediate correlation times [22].

1. The FitzHugh–Nagumo system driven by dichotomic noise

Let us study an 2d-array of units with FitzHugh–Nagumo (FHN) kinetics obeying the equations:

$$\frac{dx_i}{dt} = x_i - x_i^3 - y_i + D_x \Delta x_i, \tag{1}$$

$$\frac{dy_i}{dt} = \varepsilon \left(x_i - a y_i - I_i(t)\right) + D_y \Delta y_i. \tag{2}$$

Here Δ denotes the discrete Laplace operator which in our numerical simulations we treated with the help of the Crank–Nicholson scheme. They stand for diffusion with constants $D_x = 0.02$ and $D_y = 5.0$ which we use unless mentioned otherwise. $\varepsilon = 0.05$ is a small parameter ensuring a timescale separation of the activator x (fast) and the inhibitor y (slow). We put the value of a to 1.475.

The random telegraph process $I_i(t)$ takes one of the two values d and $-d$. Switching between the two states occur with rate γ and the correlation function of the process is given by

$$\langle I_i(t_1) I_j(t_2) \rangle = d^2 e^{-2\gamma|\tau|} K(i,j) \tag{3}$$

with $\tau = t_2 - t_1$ and $K(i,j)$ is the spatial correlation function between the different sites in the array.

The dynamics of a single FHN system results putting $D_x = D_y = 0$. Setting additionally $I(t)$ to one of the values, for example $I(t) = d$, the system becomes deterministic. For large enough $|d|$ ($|d| > d_c = 2a\sqrt{\frac{1}{27}(1 - \frac{1}{a})} \approx 0.104$) this FHN system exhibits excitability. A (single) stable fixed point exists such that small perturbations around it decay. Perturbations exceeding a certain threshold lead to a large excursion of a unit in phase space before the excursion returns to the single fixed point again. With smaller $|d| < d_c$ the FHN system exhibits bistability, i.e. it possesses two stable and one unstable fixed point. Later on, the forcing is always overcritical, i.e. $|d| > d_c$.

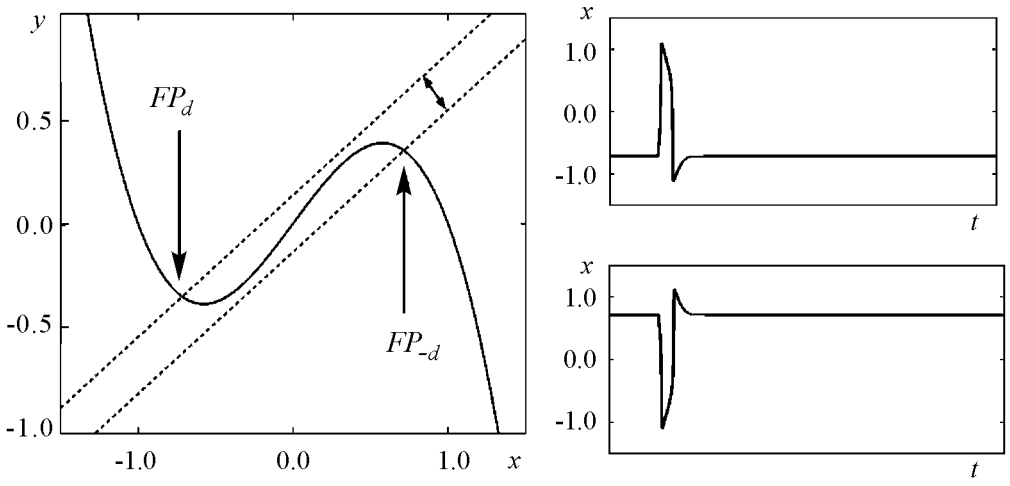

Fig. 1. Left graph: Nullclines of a single FHN-System: Activator nullcline (solid line) obtained by setting $\dot{x} = 0$, inhibitor nullclines (dashed lines) obtained by setting $\dot{y} = 0$ and shown for the two different realizations of the dichotomic driving $I(t) = \pm d$. The FP_i label the different fixed points. Right graphs: Dynamics of $x(t)$ for $d = 0.2$ (upper plot) and $d = -0.2$ (lower plot) with single spikes after a superthreshold perturbation

A single system is in another excitable regime with equivalent dynamics for $I(t) = -d$. Its easily seen and due to the symmetry of Eqs. (1),(2) under the transformations $x \to -x$ and $y \to -y$. Therefore, switching between the two states $\pm d$ of the random telegraph process $I(t)$ realizes transitions between two excitable dynamical regimes of the FHN system (1),(2) associated with either the fixed point located on the left or on the right branch of the cubic nullcline, respectively. A corresponding graphical interpretation is presented in Fig. 1.

2. Global alterations

First we assume a spatially uniform driving, i.e. $K(i, j) = 1$ and a global dichotomic switching is applied to the system ($I_i(t) = I(t)$). We denote the dynamics of the lattice system (1), (2) by

$$\dot{\mathbf{x}}_{\pm d} = \begin{pmatrix} \dot{x} \\ \dot{y}_{\pm d} \end{pmatrix}. \tag{4}$$

Corresponding fixed points are called $\mathbf{x}_{0,+d}$ and $\mathbf{x}_{0,-d}$, respectively. The system was initialized in the dynamical regime $\dot{\mathbf{x}}_{+d}$ with the initial values of the units $(x_n(0), y_n(0))$ at the corresponding fixed point $\mathbf{x}_{0,+d}$. In space this corresponds to a homogeneous steady state. In our numerical simulations we add tiny but crucial Gaussian white noise of intensity 10^{-6} (for comparison: d is of order 10^{-1}) to the system by reason to provide an almost homogeneous distribution of the units around the resting position. Hereafter we will refer to this set of points with coordinates $(x(t), y(t))$ as the cloud. In space the coupled units in the cloud still shape as a virtually homogeneous steady pattern.

2.1. Low Switching Rates. First we study the dynamics of a $1 - d$ system for a very low switching rate γ. The mean time between two switchings is larger than the relaxation time to the two fixed points $\propto (\varepsilon a)^{-1}$. In what happens there will be enough time left in between two consecutive switchings that units can travel from one branch of

the cubic nullcline to the other. In the ideal case the whole cloud stays at the fixed point $\mathbf{x}_{0,d}$ for a very long time keeping the lattice state close to the homogeneous steady state. Once a switching $d \to -d$ occurs the cloud leaves this fixed point for $\mathbf{x}_{0,-d}$ approaching its counterpart where then all the members of the cloud remain captured in the vicinity of this fixed point until the next switching $-d \to d$ occurs and the transition process starts all over again.

2.2. Intermediate Switching Rates. A different behavior was found for higher switching rates γ. After some passages of the cloud back and forth inhomogeneous structures are formed as illustrated in Figs 2 and 3.

The emerging patterns are the product of a switching of the telegraph signal taking place just at the moment when the cloud has begun to cross the excitation threshold. Some individual units of the cloud are already beyond the threshold moving to the left. They will get excited executing a swift transition to the left outer branch of the cubic nullcline. The remaining units that lag behind, return to the nearby fixed point on the right branch which appears as result of the second back switching. But, crucially, units arriving at the left outer branch of the cubic nullcline get trapped there due to the strong inhibitory coupling (vertical direction) that prevents their passage downwards the left cubic nullcline with subsequent return to the right part of the cubic nullcline. This trapping feature, being crucial for the pattern formation, has to be distinguished from the behavior without diffusive coupling, i.e. when $D_x = D_y = 0$. It realizes a Turing like instability.

In the corresponding time series a single spatial hump occurs (see Fig. 1). In contrast to the uncoupled case, with proper inhibitory coupling (a small ratio D_x/D_y is mandatory) the units become trapped on the left outer branch of the cubic nullcline. Such hump arrange in space that a large-amplitude spatial inhomogeneity is attained. It resembles the shape of a localized stationary pattern (also referred to as a *contrast structure*) being characteristic for excitable media [23–26]. The position on the lattice at which the the first hump appears is arbitrary. It depends on that part of the randomly distributed units in the cloud which is beyond the excitation threshold at the switching moment. As was demonstrated in [24, 28] this stationary pattern is stable with respect to small perturbations but the spatial structure possesses a Goldstone mode and can freely diffuse in space.

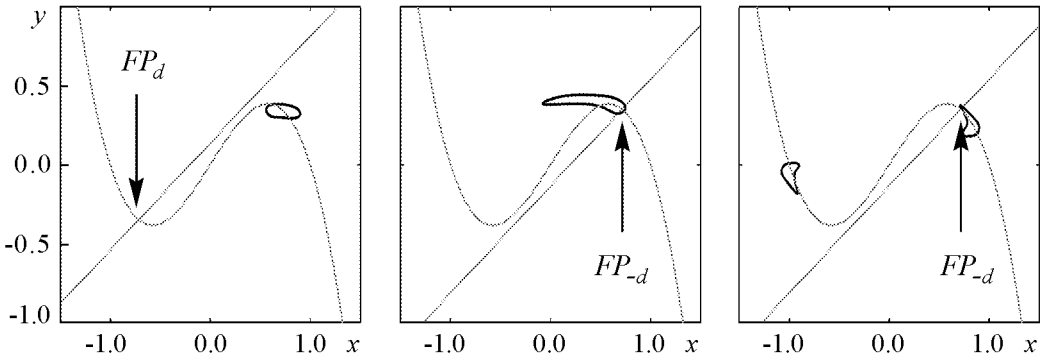

Fig. 2. Development of stationary inhomogeneous patterns in phase space x, y for medium switching rates. Initially distributed with small inhomogeneities (indicated as a cloud) is initially distributed around a fixed point. Once a switching occurs (left panel) the cloud starts to move to the second fixed point. If a second switching occurs just as the cloud is passing from the left to the right (middle panel) the cloud can be split into two. The second cloud then does not return to the fixed point of the deterministic system but moves to the other side fixed by inhibitor diffusion. A spatial structure is formed (cf. Fig. 3)

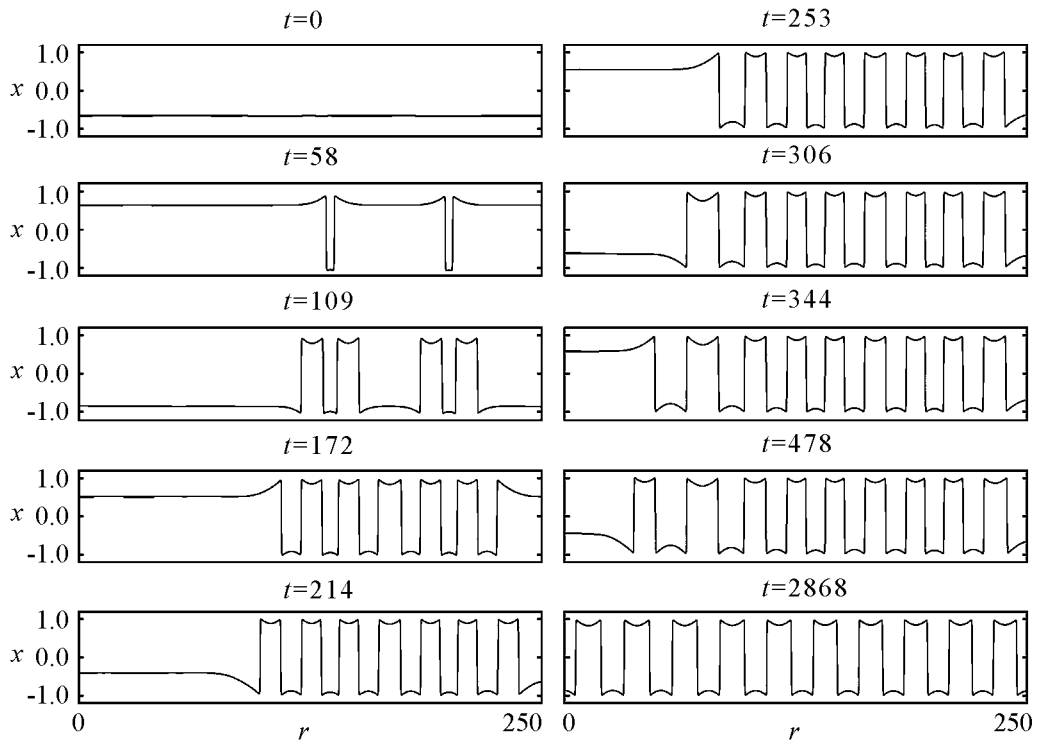

Fig.3. Development of stationary patterns for medium switching rates - real space. The activator distributions $x(r)$ as functions of space is presented for several times t. After the first nuclei was formed every switching of the homogeneous part of the cloud from one fixed point to the other adds a new layer at either side of this nucleus. After a long time a very regular structure is formed. The time is given above each picture. The y–variable (not shown) oscillates with equal period but small amplitude [23]. No-flux boundary conditions are used. The lattice constant is 0.05

Such large spatial inhomogeneity can be called a *nucleus*. At each further switching of the homogeneous regions, adjacent to the nucleus new local humps are built up as is illustrated in Fig. 3. With each switching the inhomogeneous region grows on the expense of the homogeneous region. The formation process goes on adding hump by hump until a periodic pattern covers the whole lattice. Eventually, the diffusive interaction between the neighboring sites leads to the formation of a perfectly periodic pattern and slight deviations in the width of the individual spatial inhomogeneities at early stages of the formation process will be dropped. However, it takes diffusion a much longer time to render the pattern regular than it took the pattern to be generated (right lower panel in Fig. 3).

It is also possible to add not only one half of a hump at each switching but also three, five, and more halves (The parameter range for adding simultaneously several layers is very small). This can for example be achieved by a change of the elongation d of the fluctuations. By varying d it is also possible to subtract half a hump with each switching (see Fig. 4, left). Moreover, a change in the diffusion constants can double the number of humps in the system (Fig. 4, right).

But this *multiplier* works only for small γ because immediately after the multiplication the distance between two consecutive humps might be very small. Therefore no new humps fit in between. Time until diffusion has restored the stable distance between them is large and during this time the multiplier does not work. Notice that in contrast to the case treated in Fig. 3 the pattern is not symmetric with respect to $x \to -x$. Let us call

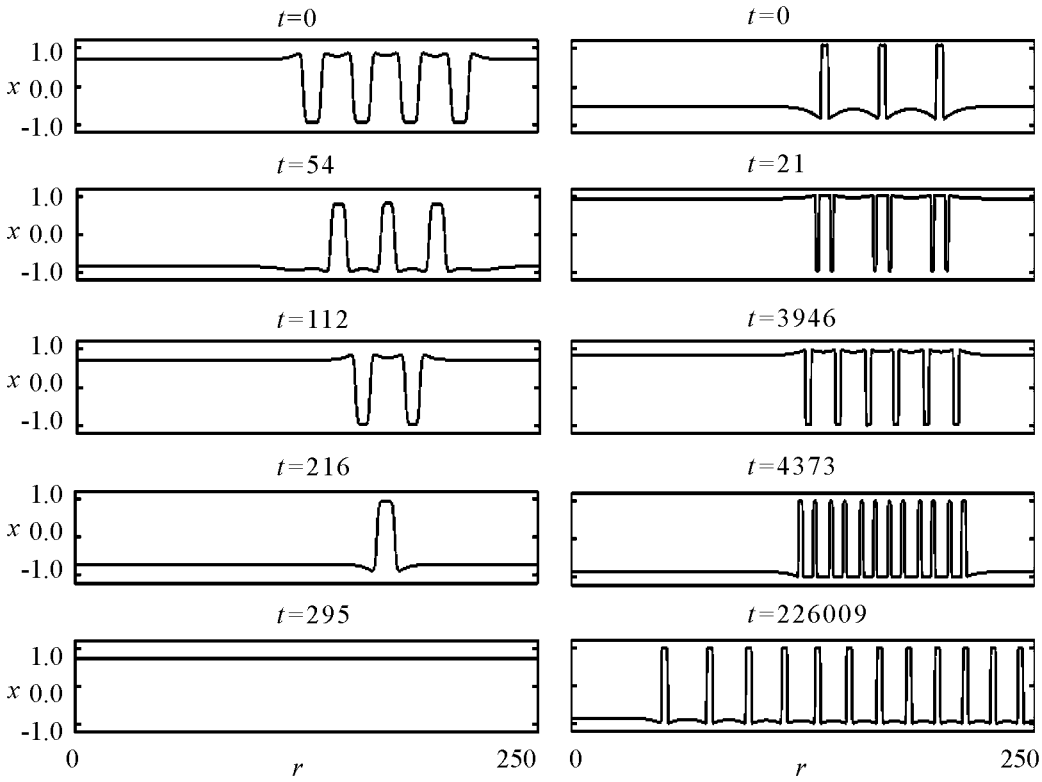

Fig. 4. Left plot: The number of humps can also be decreased ($D_x = 0.9$). Shown are snapshots shortly after each switching. Right plot:The number of humps can also be multiplied ($d = 0.5$). In this case the time between two consecutive switchings must be large enough to restore the stable distance between two neighboring humps. Switchings occur only between line one and two and between line three and four

the width of a hump l_h and the distance between two neighboring humps Δ_h. Δ_h must roughly increase to three times l_h before a new multiplication can be performed.

The final localized pattern can be studied by means of the outgoing stationary system (4) for $I = d$

$$\begin{aligned} 0 &= x_i - x_i^3 - y_i + D_x \frac{x_{i-1} - 2x_i + x_{i+1}}{\Delta r^2}, \\ 0 &= \varepsilon(x_i - a y_i + d) + D_y \frac{y_{i-1} - 2y_i + y_{i+1}}{\Delta r^2}. \end{aligned} \tag{5}$$

Let us set here the lattice spacing Δr equal to one. By defining

$$x_n = s_n, \quad x_{n-1} = t_n, \quad y_n = u_n, \quad y_{n-1} = v_n \tag{6}$$

the set of equations is equivalent to the four dimensional map

$$\begin{aligned} s_{n+1} &= \frac{1}{D_x}\left(-s_n + s_n^3 + u_n\right) + 2s_n - t_n, \\ t_{n+1} &= s_n, \\ u_{n+1} &= \frac{\varepsilon}{D_y}\left(s_n - a u_n + d\right) + 2u_n - v_n, \\ v_{n+1} &= u_n\,. \end{aligned} \tag{7}$$

Inspecting closely the periodic pattern (lower right panel in Fig. 3) we see that there exist small transition areas between large regions of almost constant amplitude. It allows to approximate the pattern as bivalued for the analytic approach.

The map (7) indeed yields bistability of a period-one (P_1) solution (homogeneous pattern) and a period-two solution (inhomogeneous pattern). The period-one solution is quickly found: We set $s_n = s_{n+1}$, $t_n = t_{n+1}$, $u_n = u_{n+1}$, and $v_n = v_{n+1}$ (this means on the lattice: $x_n = x_{n+1}$, and $y_n = y_{n+1}$) and notice that the solutions of the map are equivalent to the stationary solutions of the zero-dimensional FHN model (1), (2).

A procedure for the period-two (P_2) case by setting $s_n = s_{n+2}$, $t_n = t_{n+2}$, $u_n = u_{n+2}$, and $v_n = v_{n+2}$ was presented in [22]. An additional solutions exist with reversed sign in d as well as with exchanged values of s_n and s_{n+1} and exchanged values of u_n and u_{n+1}. The first solution (upper row) is of period one. It is the same solution as in the zero-dimensional FHN as discussed above. The second and the third solution are of period two. This fits well to the results from the reaction-diffusion simulation (Fig. 3).

In order to test the stability of the solutions we linearize Eqs (7) around the fixed points. The corresponding eigenvalue (There are two eigenvalues for each fixed point. For a stability analysis we need to study only the eigenvalue with larger real part.) is given by:

$$\begin{aligned} \lambda(k) &= \frac{1 - 3x_0^2 - \varepsilon a + 2(D_x + D_y)(\cos(k) - 1)}{2} + \\ &+ \sqrt{\frac{(1 - 3x_0^2 - \varepsilon a + 2(D_x + D_y)(\cos(k) - 1))^2}{4} - \varepsilon}. \end{aligned} \tag{8}$$

One can conclude that the period-one solution is stable as well as the period-two solution with alternating sign. The second period-two solution is unstable. Interpreting finite series of humps as a segment of the stable period-two solution and assuming that such a segment is also stable we can understand the pattern formation in terms of the map orbits: Due to the combined action of the additive noise and the dichotomous switching a finite region of the lattice is brought close to the basin of attraction of such a stable segment. With each further switching the elements at the border of the finite inhomogeneous segment are drawn towards the inhomogeneous solution.

Conclusively, we have demonstrated that global alteration between two different monostable excitable dynamics yields pattern formation while each of the monostable dynamics does not. The situation can hence be viewed as some kind of Parrondo's Game: switching between two loosing strategies constitutes a winning strategy [27].

It is noteworthy that this phenomenon can also/cannot be observed in periodically driven systems. Also we underline that the probability per unit time for the occurrence of pattern formation approaches zero as the magnitude of the inhomogeneities (size of the cloud) imposed by the tiny additive Gaussian noise on the system diminishes. Therefore the presence of inhomogeneities is vital for the dichotomously-driven mechanism of pattern formation. A growth of an initial hump might also occur for very low switching rates γ. But it takes a much longer time for the phenomenon to occur and we did not observe it in our simulations.

2.3. High Switching rate. In this subsection we focus on a high switching rate γ, respectively, on fast switchings. Such system behaves as if instead of the signal its temporal average have been applied. Consequently we put $I_i(t) \to \langle I_i(t) \rangle = 0$ in (1) and (2). In the FHN for a single system in case of the selected parameters two stable and one unstable fixed points, or bistability is established (see Fig. 5, in order to show the complexity of the dynamics we changed slightly parameters in the left panel and complex

limit cycle behavior is found). The stable ones, denoted by $\pm\mathbf{x}_{0,det}$, are symmetrically placed around the origin of phase space. Obviously, the system with diffusive coupling possesses also fixed points at these locations. However, by choosing proper coupling constants (It is important that the diffusion constant of the inhibitor y is much larger than that of the activator x.) these homogeneous fixed points may loose their stability via a diffusion induced or Turing instability. More precisely, the stability of the fixed points $\pm\mathbf{x}_{0,det}$ depends on the wavelength of the perturbation enforced on the system. The largest eigenvalue $\lambda(k)$ of the extended system linearized around the stable fixed point $\mathbf{x}_{0,det} = (\tilde{x}\ \ \tilde{y})^t$ is given by:

$$\begin{aligned}\lambda &= \frac{1}{2}\left(1 - 3\tilde{x}^2 + \tilde{D}_x + \tilde{D}_y - a\varepsilon\right) + \\ &+ \frac{1}{2}\sqrt{\left(1 - 3\tilde{x}^2 + \tilde{D}_x + \tilde{D}_y - a\varepsilon\right)^2 - 4(1 - 3\tilde{x}^2 + \tilde{D}_x)(\tilde{D}_y - a\varepsilon) - 4\varepsilon} \qquad (9)\end{aligned}$$

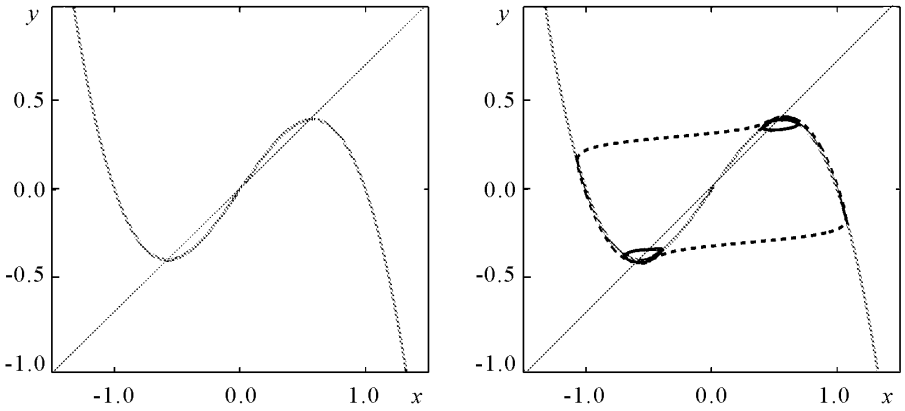

Fig.5. Left panel ($a = 1.475$): Three fixed points but no limit cycles exist. The fixed points are given by the intersections of the nullclines (solid gray). The outer points are stable, the inner is unstable. Right panel ($a = 1.46$): A slight change in the parameter leads to the development of three limit cycles. Each stable fixed point is embraced by an unstable limit cycle (solid black). All of the fixed points together with their embracing limit cycles are encircled by a large and stable limit cycle (dashed black)

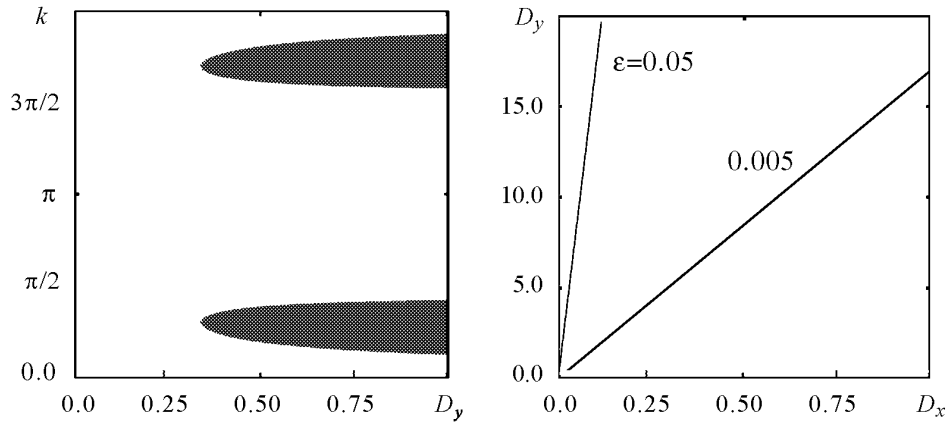

Fig. 6. Left: Regions of positive real part (black) of the eigenvalue of the linearized problem in the inhibitor coupling strength–wave vector plane. Other parameters the same as throughout the paper. Right: Region of Turing instability for different values of the timescale separation ε. The homogeneous state is unstable above the lines

with

$$\tilde{D}_{x,y} = 2D_{x,y}(\cos(k) - 1). \tag{10}$$

Fig. 6 presents regions of Turing instability in the k–D_y–plane. The instable regions with positive real parts of λ are depicted as black regions. As can be seen perturbations of a finite wavelength larger than zero are favored to grow if the inhibitor diffusion coefficient D_y becomes large. We also depict the region where Turing instabilities occur in the D_x–D_y plane. Apparently, with enhanced timescale separation (smaller ε) the Turing space is enlarged.

We demonstrate the effect of different switching rates γ in Fig. 7 for a spatially two dimensional lattice. For low and intermediate rates we have started with inhomogeneous initial conditions and for high rates with homogeneous ones. Note that inhomogeneities grow due to the combined action of global switching and small additive noise as demonstrated in Fig. 2. In all situations we applied additive Gaussian noise of intensity 10^{-6} to each individual element.

The growth of the patterns is due to three different mechanisms: For $\gamma = 0$ the instable border grows slowly into the homogeneous region. In the case of intermediate

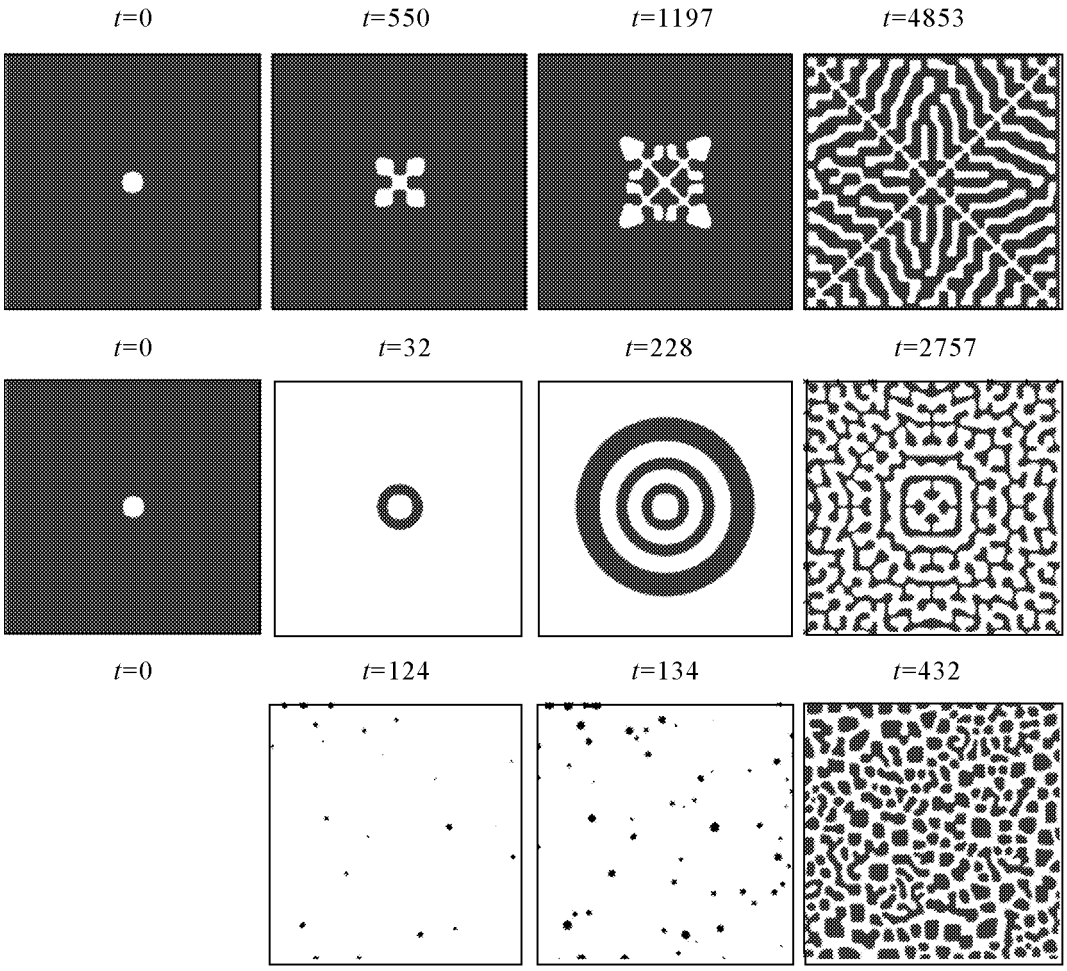

Fig.7. Time series with different switching rates. The time is given above each plot. Parameters: $\gamma = 0$ (upper row), 0.01 (middle row), 5.0 (lower row); $\varepsilon = 0.05$, $a = 1.475$, $D_x = 0.02$, $D_y = 5.0$, $d = 0.2$

γ switchings generate additional layers at the boundary. If we denote with L the period length of the final pattern in Fig. 3 we can estimate the speed of the growth of the patterns radius as follows: After the time T the process $I(t)$ has on average switched γT times. With each switching an additional layer (half a hump) is appended to the inhomogeneity. The average speed of the propagation of the boundary $\hat{v}$ is then given by $\hat{v} = (1/2)\gamma L$. This constitutes an upper limit for the average speed because switching have no effect on the growth of the pattern if they occur too early, i.e. before the homogeneous part is in the vicinity of a fixed point. Simulations with different parameter values showed that it is also possible to add instead of one half a layer three, five, or more halves at each side of the inhomogeneity. Also, it is possible to decrease the size of the inhomogeneity. The average speed of propagation is therefore more generally given by:

$$\bar{v} = \left(\frac{1}{2} + Z\right)\gamma L, \tag{11}$$

where Z is an integer number that depends on the parameters of the system (L also depends on the parameters).

For high γ inhomogeneities grow all over the array. The speed with which the patterns grow is therefore different for the three cases: the faster the switching, the faster the growth.

3. Frozen noise

A quite interesting case is the limit of vanishing switching rates of the random telegraph signal. It corresponds to a static dichotomous disorder in the system. Besides the value of the amplitudes d the spatial correlation of the randomness signal is the new important parameter. We will control these in a simple way via the lattice spacing used in our simulation.

A certain realization of static dichotomous disorder in a two-dimensional lattice system is shown in the left panel of Fig. 8. The two dimensional plane is divided into 400×400 pixel and for every pixel a random generator selects the two possible values, $\pm d$. The right panel of Fig. 8 shows the results of a numerical simulation with that noise realization. As in the case of fast global switching we see a Turing pattern emerge. The pattern is not a mere reflection of the underlying disorder but has a structure of it's own. It's typical wavelength is much larger than that of the disorder. As initial conditions we chose $x_i = 0.56748$ and $y_i = 0.384732$ for all $i = 1, ..., N$. This is the location of the stable fixed point of a single system without dichotomous driving ($I_i = 0$). The dynamical process of pattern formation is again driven by a Turing instability. Perturbations of a certain critical wavelength grow until they form the pattern shown in Fig 8.

The pattern formation takes place in 2-d as well in 1-d. Typically, Turing patterns in 2-d come in two different shapes ([1]): In labyrinth- and in hexagonal shape. With our study we found that the lattice system of Eqs (1), (2) supports only the labyrinth type.

We have investigated numerically different samples with the same lattice constant but with frozen dichotomous signals of different typical wavelength. Particularly illuminating are in parameter regions where the homogeneous deterministic system ($I_i(t) = 0$) does not support pattern formation. Such situation is realized by reducing the inhibitor coupling coefficient to $D_y = 0.5$ which stabilizes the fixed points.

Very fine dichotomic noise realization, i.e. one with a small typical length $l \propto \Delta r$ generates as expected not a new behavior. The system response remains equivalent to that of the deterministic system and a homogeneous distribution in the fixed point is established (upper row in Fig. 9). In contrast, with coarser dichotomic perturbation we observe the excitation of stationary patterns form (lower line in Fig. 9). We can thus by changing the correlation length of the disorder increase generate Turing patterns. It would allow to reduce significantly the ratio between activator and inhibitor diffusion constants.

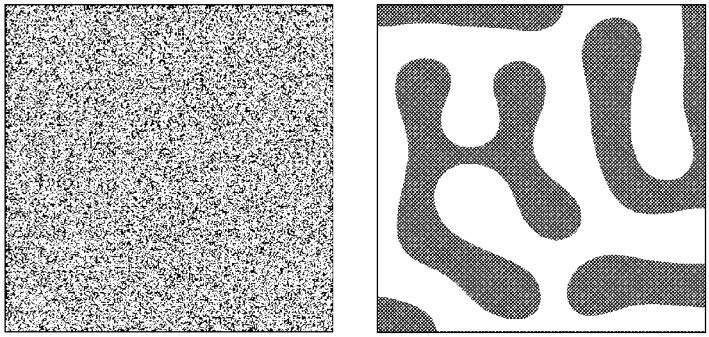

Fig. 8. Turing pattern (right) obtained by applying frozen dichotomic disorder (left) to a homogeneous system at the fixed point. $K(i,j) = \delta_{i,j}$; Size: 400×400; $\Delta r = 0.1$; $d = 0.2$. Left graph shows frozen disorder $I_{i,j}$ and right one shows response of the FHN

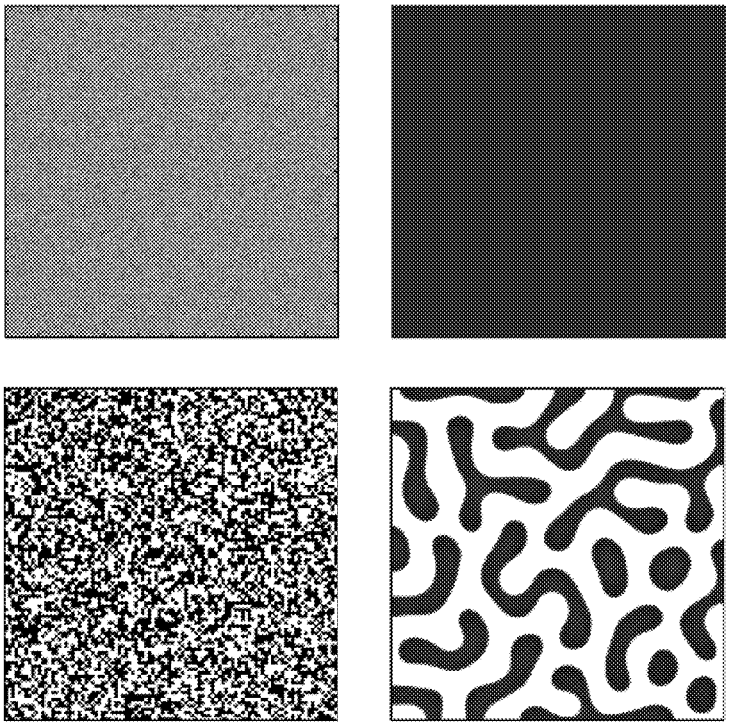

Fig. 9. Coarse fluctuations support pattern formation, fine ones do not. In this parameter regime the system with $I_{ij}(t) + \mathrm{const}$ does not support Turing pattern formation. $D_y = 0.5$, $\Delta r = 0.02$, $l = 1$ (upper row) and $l = 20$ (lower row). 2000×2000 points are shown. Left graphs show frozen disorder $I_{i,j}$ and right ones show response of the FHN

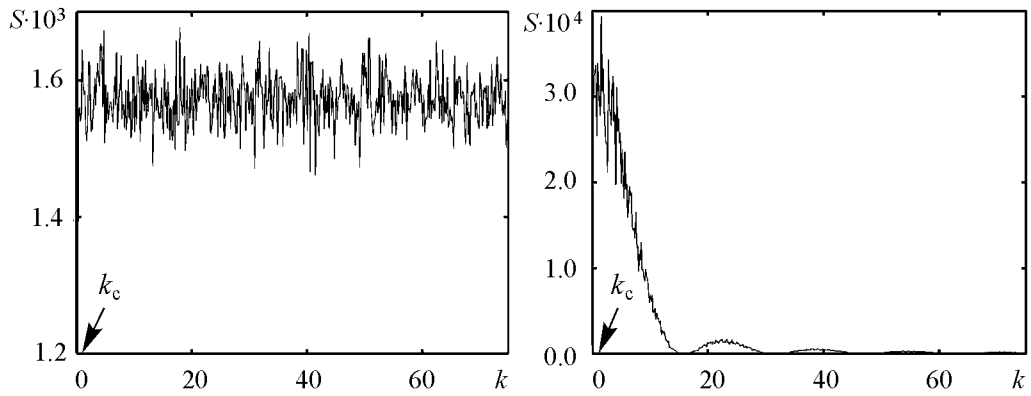

Fig.10. Structure factor $S(k)$ of the underlying noise for the patterns in Fig. 9. The left panel corresponds to the fine disorder in Fig. 9 (upper row), the right to the coarse disorder (lower row)

The role of large correlation length of the disorder can be inspected by looking at its structure factor $S(k)$ in 1-d. It is given by the Fourier transform of the spatial correlation function. In [22] we have derived for the spatial correlation function

$$\langle I_i\, I_j \rangle = K_{i,j} = d^2 \left(1 - \frac{|i-j|}{l} \right). \tag{12}$$

Afterwards the structure function reads

$$S(k) = \frac{2d^2}{lk^2} \left(1 - \cos(kl) \right). \tag{13}$$

We show plots of both in Fig. 10. We underline that modes with the critical wavenumber k_c gain much higher power in the case of the large correlation length compared for the small correlation length. This is a possible reason for the formation of the patterns. The high power at k_c may lead to a larger amplitude of the deviations from the steady state of wavelength k_c and destabilize the homogeneous state by driving the system into the nonlinear regime.

Conclusions

The influence of additive temporal and spatial dichotomous perturbations in a diffusively coupled array of the FitzHugh–Nagumo system was studied numerically. Perturbations were chosen such that locally with fixed dichotomous drive one of two excitable dynamics was realized. We emphasize that in both cases $I = \pm d$ there exists a stable homogeneous steady state. We have shown that due to appropriate switching between the two dynamical regimes either of the two steady states can be destabilized. This effect depends on the diffusion constants of the activator x and the inhibitor y and of the amplitude of the driving.

In case of global alterations and intermediate switching rate we have found a new mechanism to create spatial structures. It proceeds via creating a stable nucleus from which the periodic pattern grows layer by layer at every switch. Change of the parameters might reverse the process and the structure shrinks back to the overall homogeneous state.

Applying frozen dichotomous disorder of finite nonzero correlation length causes destabilization of homogeneous steady states leading again to Turing patterns. This holds even for parameter values for which the dynamics obtained by spatiotemporal averaging of I as performed in [16] does not sustain Turing instability.

References

1. *Koch A.J., and Meinhardt H.* Biological pattern formation: from basic mechanisms to complex strucctures // Rev. of Mod. Phys. 1994. Vol. 66. P. 1481.
2. *Mikhailov A.S.* Foundations of Synergetics I. 2nd Ed. Springer, Berlin-Heidelberg, New York, 1994.
3. *Garcia-Ojalvo J., and Sancho J.M.* Noise in Spatially Extended Systems. Springer-Verlag, New York, 1999.
4. *Anishchenko V., Neiman A., Astakhov A., Vadivasova T. and Schimansky-Geier L.* Chaotic and Stochastic Processes in Dynamic Systems. Springer, Berlin-Heidelberg-New York, 2002.
5. *Lindner B., Garcia-Ojalvo J., Neiman A., and Schimansky-Geier L.* // Phys. Rep. 2004. Vol. 392. 321.
6. *Sagues F., Sancho J.M., and Garcia-Ojalvo J.* // Rev. Mod. Phys. 2008.
7. *Mikhailov A.S.* // Z. Phys. B. 1981. Vol. 41. 277.
8. *Garcia-Ojalvo J., and Sancho J.M., and Ramirez-Piscina L.* // Phys. Lett. A. 1992. Vol. 168. 35.
9. *Parrondo J.M.R., C. van den Broeck, Buceta J., and F.J. de la Rubia.* // Physica A. 1996. Vol. 224. 153.
10. *Zaikin A.A. and Schimansky-Geier L.* // Phys. Rev. E. 1998. Vol. 58. P. 4355.
11. *Kawai R., Sailer X., Schimansky-Geier L., and Van den Broeck C.* Macroscopic limit cycle via pure noise-induced phase transitions // Phys. Rev. E. 2004. Vol. 69. 051104.
12. *Buceta J., Ibanes M., Sancho J.M., and Lindenberg K.* // Phys. Rev. E. 2003. Vol. 67. 021113.
13. *Buceta J., Lindenberg K., and Parrondo J.M.R.* Stationary and oscillatory spatial patterns induced by global periodic switching // Phys. Rev. Lett. 2002. Vol. 88. 024103.
14. *Buceta J., Lindenberg K., and Parrondo J.M.R.* // Phys. Rev. E. 2002. Vol. 66. 036216.
15. *Buceta J., and Lindenberg K.* // Phys. Rev. E. 2002. Vol. 66. 046202.
16. *Buceta J. and Lindenberg K.* Spatial patterns induced purely by dichotomous disorder // Phys. Rev. E. 2003. Vol. 68. 011103.
17. *FitzHugh R.* // Biophys. J. 1961. Vol. 1. 445.
18. *Nagumo J. and Arimoto S. and Yoshitzawa S.* // Proc. IRE. 1962. Vol. 50. 2061.
19. *Vasilev V.A., Romanovski Yu.M., and Yakhno V.G.* // Uspekhi Fiz. Nauk. 1979. Vol. 128. 626.
20. *Elphick C., Hagberg A., and Meron E.* Dynamic front transitions and spiral-vortex nucleation // Phys. Rev. E. 1995. Vol. 51. 3052.
21. *Martinez K., Lin A.L., Kharrazian R., Sailer X., and Swinney H.L.* Resonance in periodically inhibited reaction-diffusion systems // Physica D. 2002. Vol. 168. 1.
22. *Sailer X.R., Hennig D., Engel H., and Schimansky-Geier L.* // Phys. Rev. E. 2006. Vol. 73. 056209.

23. *Koga S. and Kuramoto Y.* Localized patterns in reaction-diffusin systems // Prog. of Theor. Phys. 1980. Vol. 63. 106.
24. *Rinzel J. and Keller J.B.* Traveling wave solutions of nerve conduction equation // Biophys. J. 1973. Vol. 13. 1313.
25. *Ohta T., Mimura M., and Kobayashi R.* Higher-dimensional localized patterns in excitable media // Physica D. 1989. Vol. 34. 1115.
26. *Ohta T., Ito A., and Tetsuka A.* Self-organization in an excitable reaction-diffusion system: Synchronization of oscillatory domains in one dimension // Phys. Rev. A. 1990. Vol. 42. 3225.
27. *Harmer G.P. and Abott D.* Losing strategies can win by Parrondo's paradox // Nature (London). 1999. Vol. 199. 402.
28. *Schimansky-Geier L., Hempel H., Bartussek R. and Zülicke C.* // Z. Physik B. 1995. Vol. 96. 417.

Поступила в редакцию 8.07.2009

СТРУКТУРЫ ВОЗБУДИМОЙ ДИНАМИКИ ПОД ДЕЙСТВИЕМ АДДИТИВНОГО ДИХОТОМИЧЕСКОГО ШУМА

X. Sailer, D. Hennig, and L. Schimansky-Geier

Формирование структур в присутствии аддитивных дихотомических флуктуаций исследуется в распределенной системе с диффузионной связью и с бистабильной кинетикой ФитцХью–Нагумо. Флуктуации изменяются в пространстве и/или во времени, являясь, беспорядком или шумом, соответственно. В отсутствие возмущений динамика не приводит к формированию структур. Однако с введением соответствующих дихотомических флуктуаций однородное стационарное состояние теряет устойчивость либо путем неустойчивости Тьюринга, либо флуктуации создают пространственные ядра неустойчивых состояний. Для чисто статического дихотомического беспорядка можно наблюдать потерю устойчивости однородных состояний для конечной ненулевой величины корреляции беспорядка, которая вновь приводит к возникновению пространственных структур.

Ключевые слова: ФитцХью–Нагумо, Turing pattern, дихотомический шум, аддитивный шум.

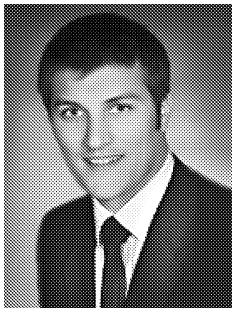

Dr. Franz Xaver Sailer 2006–2009 Investment Banking Nomura International Plc; 2001–2006 PhD Studies Humboldt Universität zu Berlin; 2000–2001 Physics Graduate Studies Master Degree University of Texas at Austin; 1997–2000 Physics Undergraduate Studies Bayerische Julius-Maximilian-Universität Würzburg; 1995–1997 Reserveoffizierausbildung; 1995 Abitur Modellschule Obersberg, Bad Hersfeld.

Newtonstrasse 15, D-12489 Berlin, Germany
Institut für Physik

Dr. Dirk Hennig was born on 1962. 1989 – Diploma of Physics, University of Leipzig. 1992 – PhD Hunboldt-University at Berlin. 1997 – Habilitation in Theoretical Physics, Free University Berlin. 1997–2002 Heisenberg Stipendiat. Award of the Teaching Authority in Theoretical Physics (Privatdozent), Free University Berlin (2001) and Humboldt University at Berlin (2008). Since 2009 – Senior Lecturer, Department of Mathematics, University of Portsmouth, UK. His main research interests are in Nonlinear Dynamics. His scientific interests include nonlinear and stochastic dynamics with application to biophysical problems and neurobiology; analytical and numerical methods for the treatment of networks of coupled nonlinear oscillators and Langevin systems. He has about seventy original publications and one review article on waves in nonlinear lattices.

Lion Gate Building, Lion Terrace, Portsmouth, PO1 3HF, UK
Department of Mathematics, University of Portsmouth

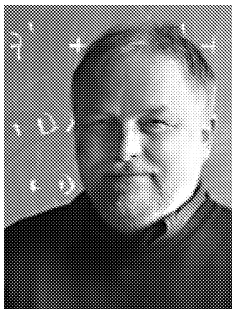

Prof. Dr. Lutz Schimansky-Geier was born on 1950. 1974 – Diploma in Physics at State University Yerevan. 1981 – PhD, 1986 – DSc Humboldt-University at Berlin. Since 1994 – Professor for Theoretical Physics.

He has about 180 original publications on: stochastic resonance, synchronization and ratchets, applications to computational neuroscience, modelization of biological motions and cellular transport, 8 book editions and 2 monographs.

Speaker of the DFG-Sfb 555 «Nonlinear Complex Processes»; Chairman of ESF Programme: «Stochastic Dynamics: Fundamentals and Applications»; Associated member of Center of Neurodynamics at UMSL, St. Louis (MO); Editor: «Fluctuation and Noise Letters» (Executive 2000–2003), «New Journal of Physics» (2008–2009), European Journ. of Physics B (since 2008).

Newtonstrasse 15, D-12489 Berlin, Germany
Institut für Physik
E-mail: alsg@physik.hu-berlin.de